Rolled-Up Nanoporous Membranes by Nanoimprint Lithography and Strain Engineering

Jaehyun Park[1], ChangKyu Yoon[2], Qianru Jin[1], Lei Chen[3] and David H. Gracias[1,2]

[1]Department of Chemical and Biomolecular Engineering, [2]Department of Materials Science and Engineering, The Johns Hopkins University, Baltimore, Maryland 21218, USA, [3]Center for Nanoscale Science and Technology, National Institute of Standards and Technology, Gaithersburg, Maryland 20899, USA

***Abstract*— It is extremely challenging to enable nanoscale patterning in three dimensional (3D) curved geometries using conventional nanolithographic approaches. In this paper, we describe a highly parallel approach that combines nanoimprint lithography (NIL) and thin film bilayer strain engineering to spontaneously roll-up nanopatterned membranes into curved geometries. Specifically, we first patterned a silicon nitride (Si_3N_4) / silicon (Si) bilayer using nanoimprint lithography followed by plasma etching to create well defined pores. The diameter of the pores was further reduced by physical vapor deposition of platinum to sizes as small as 50 nm. After patterning, the bilayers were released from the substrate by etching an underlying SiO_2 sacrificial layer. Based on the high deposition stress values for low pressure chemical vapor deposition (LPCVD) deposited Si_3N_4 and Si, we varied the thickness of the bilayer to realize rolled-up tubes with different radii of curvature; these curvature values were in good agreement with a finite element analysis model (FEM). The assembled nanoporous tubes had well defined pores along their curved interface and can be applied for drug delivery, separations and ion-sensing devices. We highlight biocompatibility of the devices by encapsulating β-TC-6 islet cells of relevance to cell encapsulation therapy for diabetes. More broadly, we believe that this approach of combining NIL with strain engineering processes could be utilized to create a range of precisely nanopatterned curved structures in a highly parallel manner.**

Keywords—Self-folding; NEMS; 3D; origami

Ⅰ. INTRODUCTION

Nanoscale patterning approaches based on electron beam or nanoimprint lithography (NIL) have revolutionized science and engineering [1]. However these approaches are typically implemented on flat planar substrates; hence it can be very challenging to realize precise nanoscale patterns in curved geometries. In order to address this challenge, focused ion beam approaches have been developed but they are inherently serial and expensive for nanomanufacturing [2]. Parallel approaches such as roll-to-roll nanoimprint lithography have been used to pattern nanoscale gratings and polarizers [3]. However, these can be challenging to implement when patterning the entire circumferential surface area of cylinders or tubes, as achieved in our present demonstration. Moreover, in many applications multiple layers of patterning are needed with registry and these patterns can be extremely challenging to implement in a roll- to-roll manner.

An emerging approach for 3D nanomanufacturing is based on the utilization of stress to curve previously lithographically nanopatterned thin films [4-10]. In one embodiment of this approach, bilayers are deposited with differential stress and then subsequently patterned using conventional planar lithographic approaches. On release from the substrate, the films relax and the strain mismatch causes them to curve spontaneously. As we demonstrate, when combined with NIL, the attractive feature of our approach is that both patterning and assembly can be realized in a highly parallel manner which is important for cost-effective nanomanufacturing.

High stresses can develop in thin films during or after deposition due to a variety of reasons such as epitaxial mismatch, thermal coefficient mismatch or defects during film growth [11]. Si_3N_4 is a silicon-based material compatible with conventional semiconductor nanofabrication technology, and is also generally considered biocompatible [12]. Therefore, Si_3N_4 is widely utilized in conventional MEMS and NEMS processing for a range of applications including electronics, sensors and biomedical engineering. Due to these attractive material properties, the nanoporous Si_3N_4 based devices that we describe are relevant for selective separations, biosensors and immunoisolation [13]. Stoichiometric LPCVD of Si_3N_4 is known to deposit films with high stress (~ 1GPa), which is required for our assembly approach, even if the high stress is avoided in many other conventional thin film applications. As the second component of the bilayer, we utilize the monocrystalline silicon (Si) device layer on commercial Silicon on Insulator (SOI) wafers.

Si is also a widely utilized material in electronics and biomedical devices and has a significantly lower stress as compared to Si_3N_4 [14]; consequently, due to this difference in stress between the two layers a strain mismatch occurs on release from the substrate. In addition, release of the bilayer can be achieved by etching the underlying buried oxide (SiO_2) layer in hydrofluoric acid with sufficiently high etch selectivity so as not to damage the patterned Si_3N_4 and Si layers.

Ⅱ. EXPERIMENTAL METHODS AND RESULTS

Nanoporous Si_3N_4/Si bilayers were first patterned on planar substrates (Fig. 1). The Si_3N_4 layer was deposited using LPCVD on an SOI wafer with a 500 nm top Si device layer. The advantage of using SOI wafers is the presence of a high quality electrically tunable Si device layer and the buried oxide layer which can serve as a sacrificial layer and be dissolved to release high quality silicon devices [15]. Hence, in principle even electronic devices patterned in the high quality tunable, semiconducting Si device layer on an SOI wafer could be formed. The LPCVD deposited Si_3N_4 and Si device layer form the mismatched strain bilayer in our experiments.

We patterned the nanopores by first spin coating a 400 nm thick thermal resist (NXR-1020, Nanonex, Fig. 1a). Periodic circular patterns were imprinted using commercial Si master molds (LightSmyth) and the Nanonex Advanced Nanoimprint Tool NX-2000 (Fig. 1b). After NIL, we performed an O_2 plasma etch (Unaxis 790 RIE) to remove the NXR-1020 thermal resist residue (Fig. 1c). Then a 50 nm thick chromium (Cr) film was deposited by thermal evaporation (Fig. 1d); the Cr serves as a dry etch mask. We dissolved the NXR-1020 thermal resist by sonication in acetone (Fig. 1e) and then dry etched the exposed Si_3N_4/Si using a Unaxis 790 RIE tool to form the nanopores. We used an etch gas composition of 1:16 of SF_6:CF_4 to etch the pores through the bilayer. Finally the

Cr was stripped using a commercial Cr etchant (CRE-473, Transene) (Fig. 1f).

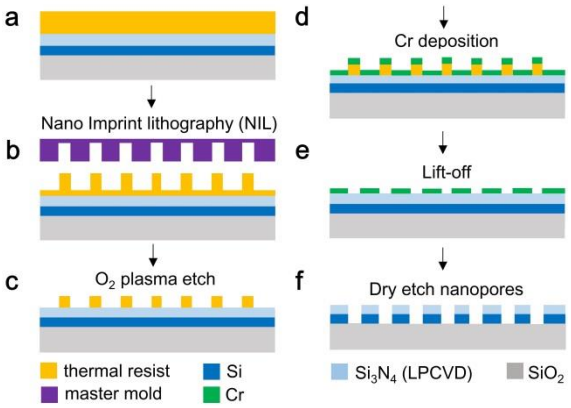

Fig. 1. Schematic of the process flow that was used to pattern the nanopores in the Si_3N_4/Si bilayer.

The NIL patterned and dry etched pores were characterized using SEM (Fig. 2). As seen, pores are well defined and have an average diameter ranging from 200 to 400 nm along the height of the pore (Fig. 2a, 2b) compared to a 200 to 290 nm diameter of the posts in the NIL stamp, as specified by the vendor; hence, the pattern was transferred with good accuracy by NIL. In case of Fig. 2c, we did observe some etch related widening of the pores in the Si layer; we attribute this widening to etch rate differences for the two different materials (Si_3N_4 and Si) of the bilayer. If needed, the undercut can be reduced by adjusting the etch parameters as seen in the SEM image of narrow pores in Fig. 2d.

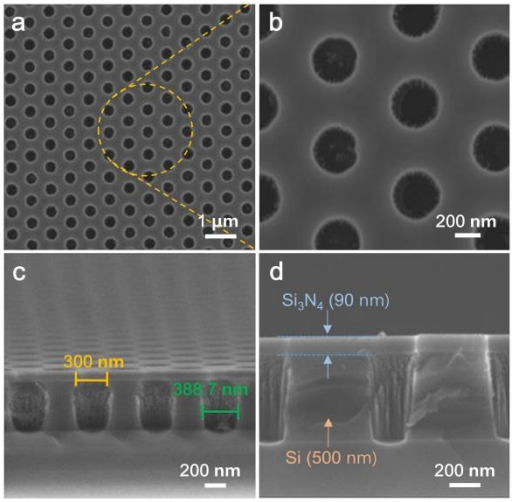

Fig. 2. SEM images of nanopores in the Si_3N_4/Si bilayer. (a) Array and (b) zoomed-in image showing well-formed pores. (c) Typical cross-section view of the nanopores, and (d) zoomed in image of pores in Si_3N_4 (t= 90 nm) /Si (t= 500 nm) thin films. By varying etch parameters, the pore widths could be tuned between 400-200 nm as illustrated in the images in panels (c) and (d).

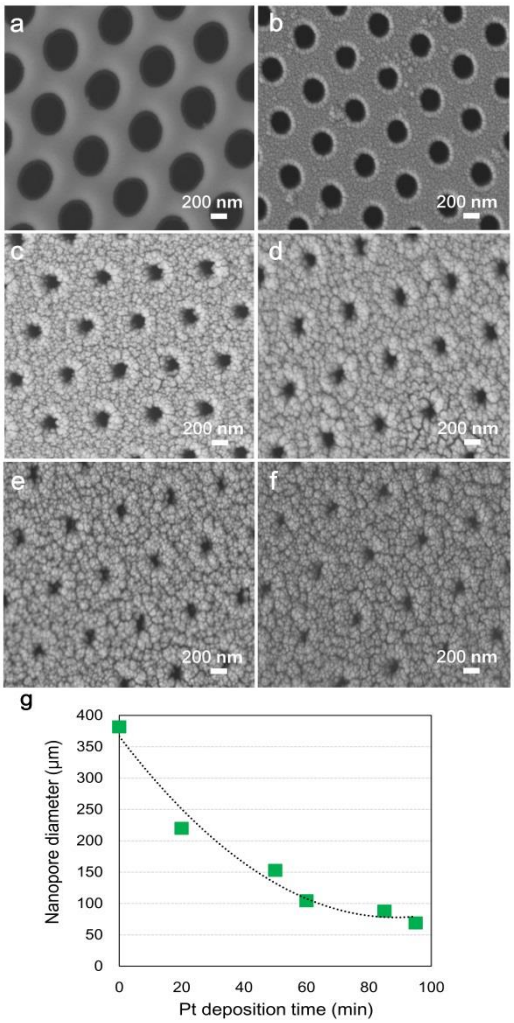

Fig. 3. Reduction in nanopore size by platinum deposition. (a-f) Pores on the rolled-up tubes with sizes ranging from an initial nanopore diameter approximately 300 nm which was decreased down to 60 nm. (g) Plot of the nanopore diameter vs Pt deposition time.

We could further decrease the pore sizes by additive deposition. Platinum (Pt) is highly biocompatible material and widely used in MEMS and NEMS fabrication especially of relevance to electrodes, electrochemical devices and biosensors [16-19]. The diameter of nanopores could be further reduced by controlling the amount of sputtered Pt. The sequence of panels in Fig. 3a to f show decreasing nanopore sizes ranging from the initial patterned nanopores (~ 300 nm) down to 60 nm when Pt was deposited for 100 minutes using power settings of 5mA and 15kV.

The schematic flow in Fig. 4a shows the process for generating 3D self- rolled tubes. The tubes are formed by releasing the strain mismatched bilayer while keeping one side attached using a patterned strip of photoresist. If needed, this strip can be dissolved to completely release the tubes from the substrate or alternatively left behind if the nanoporous tubes need to be integrated with other on-chip components such as in conventional microfluidic devices. Importantly, the assembly process is parallel (Fig. 4b) and the

zoomed in image shows well-formed tubes with NIL patterned nanoporous surfaces (Fig. 4c to 4e).

We also investigated the tunability of curvature in the roll-up process by varying several geometric parameters such as the lateral dimensions and thickness of Si_3N_4/Si bilayer. For example by controlling the width of the bilayer we can control the circumference of the tube. Hence, it is possible to assemble semi-cylinders, cylinders, and rolls with overlapping seams as shown in Fig. 5a to 5c. Further, by controlling the thickness of Si_3N_4 thin layer from 50 nm to 140 nm, the roll diameter could be varied from 200 to 500 μm.

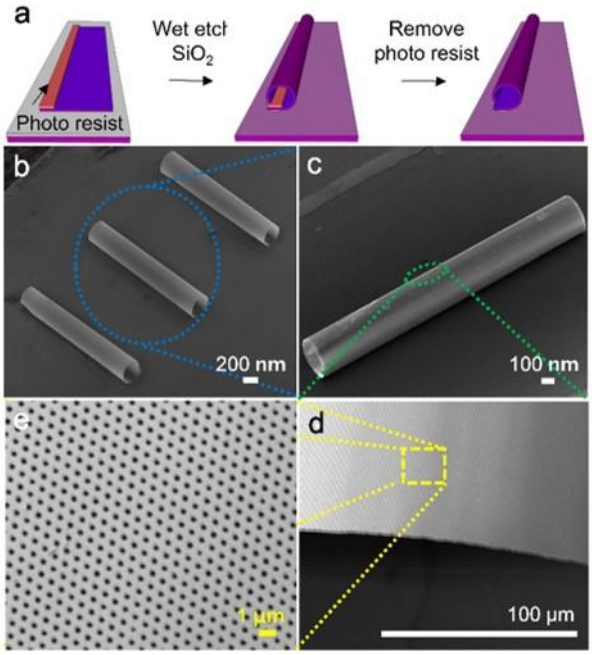

Fig. 4. Schematic and experimental images showing the (a) process flow and (b-e) SEM images of self-rolling nanoporous films. (b) Multiple and (c) single rolled-up film (d, e) Array of well-formed nanopores by NIL.

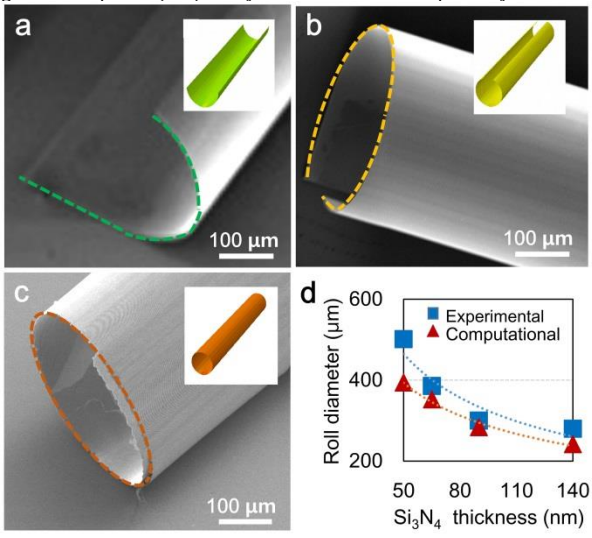

Fig. 5. Experiments and FEM results of rolled-up nanoporous membranes with different characteristics. (a-c) SEM images of semi-cylinders, cylinders and rolls with overlapping seams. (d) Plot comparing experimental and FEM curvature as a function of Si_3N_4 thickness.

In order to understand the mechanics of self-rolling and rationalize the variation in the diameter of the cylinders, we performed finite element analysis. The Si_3N_4/Si bilayer was constructed using a 3D deformable shell model in ABAQUS (Dassault Systemes), considering the large length/thickness ratio. The dimensions were selected directly from the experimental design parameters. The elastic properties and stress in LPCVD S_3N_4 films were obtained from the literature [14] and are listed in Table 1.

TABLE I. ELASITC PROPERTIES OF EACH LAYER

	Simulation parameters			
	Thickness (nm)	***Young's modulus (GPa)***	***Poisson Ratio***	***Stress (MPa)***
Si_3N_4	50 to 140	290	0.253	1000
Si	500	190	0.220	0

Since in the experiments, one edge of the thin film was fixed on the wafer using the photoresist strip, the plane strain condition was considered for this case. Therefore, for boundary conditions, we fixed one edge displacement as zero in all translational and rotational directions. We modeled the stress in Si_3N_4 by assigning a thermal expansion coefficient only in Si_3N_4 layer, and applying a temperature field to simulate the folding process. The shell is meshed by structured quadratic elements. The shell layer uses the Simpson's integration rule and each layer was assigned with nine integral points. Further, we verified that an increase in the mesh element density and integral points did not make a significant difference to the results. The model predicts similar trends to that observed in experiments. Essentially, an increased Si_3N_4 thickness from 50 to 140 nm improves the folding and yields smaller diameter tubes in agreement with experimental results (Fig. 5d). We rationalize this result by noting that the stress-thickness product is important in causing rolling and if either the stress or the thickness of the driving layer is too low, then the bending moment of the bilayer is small so the tubes formed would have large radii. However, this moment is balanced by the bending rigidity which also depends on thickness so increasing the thickness of the Si_3N_4 will eventually cause reduced bending and larger radii. Based on our simulations for the values in Table 1 and a fixed thickness of the Si layer = 500 nm, our model suggests that the maximum bending (rolling) with an associated radius of curvature of 198 μm in diameter (inflection point) would occur at a Si_3N_4 thickness of 267 nm.

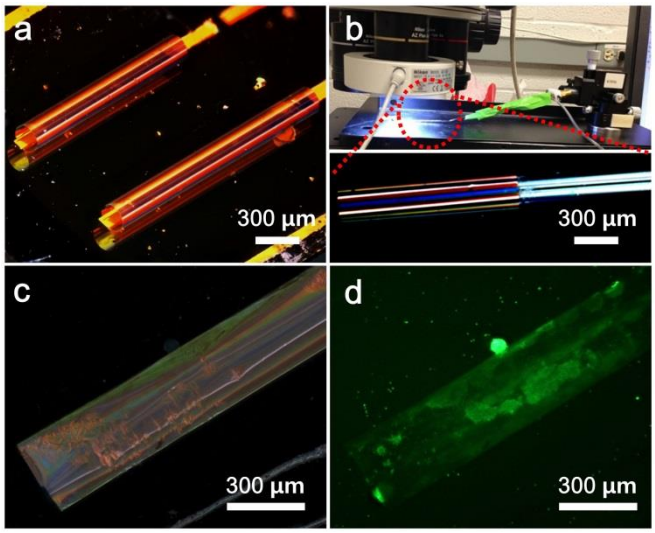

Fig. 6. Cell culture in nanoporous tubes. (a) Optical image of the rolled-up nanoporous Si_3N_4/Si bilayers and (b) experimental set-up for loading the cells into the tubes. The set-up consists of a hollow glass-tube inserted into the nanoporous tube and attached to a syringe pump for controlled loading of a high-density cell suspension (c-d) Optical and fluorescence image of calcein (viability stain) stained cells indicating cell viability.

One of the applications of nanoporous membranes is in the encapsulation and delivery of xenotrasplanted islet cells for diabetes therapy [20]. It has been suggested that nanoporous membranes could protect encapsulated cells from various components of the immune system while enabling adequate transport of nutrients, waste and therapeutic insulin from transplanted cells. A variety of nanoporous hydrogel materials such as alginate have been utilized but it has been suggested that nanofabricated pores with well-defined chemistry and straight pore geometries could enhance immunoisolation and reduce biofouling [21]. However, it can be challenging to create such 3D nanoporous capsules using conventional fabrication approaches due to the inherent planarity of parallel lithographic approaches. We explored the use of our rolled-up tubes as nanoporous encapsulants for cells and devised an experimental set-up to load *β*-TC-6 (beta) cells (ATCC, CRL-11506) into the tubes using a syringe pump (Fig. 6a and 6b). After loading, cells were cultured in the tubes and cell viability was verified after five days by staining with a Calcein stain. This stain fluoresces green in live cells due to acetoxymethyl ester hydrolysis by esterases that are present within cells. We observed that cells fluoresced green indicating cell viability in the nanoporous tubes (Fig. 6c and 6d). Further studies are needed to develop approaches to effectively seal the two ends of the tubes and measure glucose release and applicability for immunoisolation. It is noteworthy that elsewhere we have demonstrated how self-aligning surface tension driven seams can be used to seal self-folding structures [22] and these approaches along with polymer plugs could be utilized.

Ⅲ. CONCLUSION

In conclusion, we have described the use of NIL and strain engineering to create precisely nanopatterned curved nanostructures. The highlight of the approach is that it is scalable and highly parallel. As opposed to expensive serial planar patterning techniques such as e-beam lithography, NIL allows highly parallel patterning. One limitation is that registry between multiple layers in NIL patterning can be challenging, but the approach is highly relevant for periodic single layer patterns such as pores, crosses or resonators. The latter patterns are relevant for optical waveguides and metamaterials. Our studies also provide further evidence that strain engineering can be used to transform flat films into curved geometries and the highly parallel nature of the approach should be contrasted with serial 3D patterning approaches such as two-photon or ion beam machining. Hence, this approach could be applied to mass-produce curved nanopatterned electronic, optical and biomedical devices in a cost-effective manner

ACKNOWLEDGEMENT

We acknowledge support from the National Science Foundation CMMI-1200241. Research was performed in part at the NIST Center for Nanoscale Science and Technology.

Certain commercial equipment, instruments, or materials are identified in this paper to foster understanding. Such identification does not imply recommendation or endorsement by the National Institute of Standards and Technology, nor does it imply that the materials or equipment identified are necessarily the best available for the purpose.

REFERENCES

[1] S. Y. Chou, P. R. Krauss, W. Zhang, L. Guo, and L. Zhuang, "Sub-10 nm imprint lithography and applications," *Journal of Vacuum Science & Technology B*, vol. 15, pp. 2897-2904, 1997.

[2] R. M. Langford, P. M. Nellen, J. Gierak, and Y. Fu, "Focused ion beam micro-and nanoengineering," *MRS Bulletin*, vol. 32, pp. 417-423 , 2007.

[3] S. H. Ahn and L. J. Guo, "Large-area roll-to-roll and roll-to-plate nanoimprint lithography: a step toward high-throughput application of continuous nanoimprinting," *ACS Nano*, vol. 3, pp. 2304-2310, 2009.

[4] G. G. Stoney, "The tension of metallic films deposited by electrolysis," *Proceedings of the Royal Society, London A*, vol. 82, pp. 172-175, 1909.

[5] V. Y. Prinz, V. A. Seleznev, A. K. Gutakovsky, A. V. Chehovskiy, V. V. Preobrazhenskii, M. A. Putyato, and T. A. Gavrilova, "Free-standing and overgrown InGaAs/GaAs nanotubes, nanohelices and their arrays," *Physica E: Low-dimensional System and Nanostructures* , vol. 6, pp. 828-831, 2000.

[6] O. G. Schmidt and K. Eberl, "Nanotechnology: thin Solid films roll up into nanotubes," *Nature*, vol. 410, pp. 168, 2001.

[7] D. J. Bell, L. Dong, B. J. Nelson, M. Golling,, L. Zhang, and D. Grützmacher, "Fabrication and characterization of three-dimensional InGaAs/GaAs nanosprings," *Nano Letters*, vol. 6, pp. 725-729, 2006.

[8] J. Wang, M. Patel, and D. H. Gracias, "Self-assembly of three-dimensional nanoporous containers," *Nano*, vol. 4, pp. 1-5, 2009.

[9] V. B. Shenoy and D. H. Gracias, "Self-folding thin-film materials: From nanopolyhedra to graphene origami," *MRS Bulletin*, vol. 37, pp. 847-854, 2012.

[10] D. Grimm, C. C. Bof Bufon, C. Deneke, P. Atkinson, D. J. Thurmer, F. Schäffel, S. Gorantla, A. Bachmatiuk, and O. G. Schmidt, "Rolled-up nanomembranes as compact 3D architectures for field effect

transistors and fluidic sensing applications," *Nano Letters*, vol. 13, pp. 213-218, 2012.
[11] L. B. Freund and S. Suresh, "Thin film materials: stress, defect formation and surface evolution," *Cambridge University Press*, 2004.
[12] A. Neumann, T. Reske, M. Held, and K. Jahnke, "Comparative investigation of biocompatibility of various silicon nitride ceramic qualities *in vitro*," *Journal of Materials Science: Materials in Medicine*, vol. 15, pp. 1135-1140, 2004.
[13] C. L. Randall, Y. V. Kalinin, M. Jamal, A. Shah, and D. H. Gracias, "Self-folding immunoprotective cell encapsulation devices," *Nanomedicine: Nanotechnology, Biology and Medicine*, vol. 7, pp. 686-689, 2011.
[14] O. Tabata, K. Kawahata, S. Sugiyama, and I. Igarashi, "Mechanical property measurements of thin films using load-deflection of composite rectangular membrane," *Micro Electro Mechanical Systems, Proceedings, An Investigation of Micro Structures, Sensors, Actuators, Machines and Robots, IEEE*, pp. 152-156, 1989.
[15] D. H. Gracias, V. Kavthekar, J. C. Love, K. E. Paul, and G. M. Whitesides, "Fabrication of micrometer-scale, patterned polyhedra by self-assembly," *Advanced Materials*, vol. 14, pp. 235-238, 2002.
[16] W. F. Agnew, T. G. H. Yuen, D. B. McCreery, and L. A. Bullara, "Histopathologic evaluation of prolonged intracortical electrical stimulation," *Experimental Neurology*, vol. 92, pp. 162-185, 1986.
[17] P. Ekkels, X. Rottenberg, R. Puers, and H. A. C. Tilmans, "Evaluation of platinum as a structural thin film material for RF-MEMS devices," *Journal of Micromechanics and Microengineering*, vol. 19, pp. 065010.
[18] P. Tyagi, D. Postetter, D. L. Saragnese, C. L. Randall, M. A. Mirski, and D. H. Gracias, "Patternable nanowire sensors for electrochemical recording of dopamine," *Analytical Chemistry*, vol. 81, pp. 9979-9984.
[19] S. B. Brummer and M. J. Turner, "Electrical stimulation with Pt electrodes: II-Estimation of Maximum Surface Redox (Theoretical Non-Gassing) Limits," *IEEE Transactions on Biomedical Engineering*, vol. BME-24, pp. 440-443, 1977.
[20] G. Orive, R. M. Hernández, A. R. Gascón, R. Calafiore, T. M. S. Chang, P. De Vos, G. Hortelano, D. Hunkeler, I. Lacik, A. M. J. Shapiro, and J. L. Pedraz, "Cell encapsulation: promise and progress," *Nature Medicine*, vol. 9, pp. 104-107, 2003.
[21] T. A. Desai, W. H. Chu, J. K. Tu, G. M. Beattie, A. Hayek, and M. Ferrari, "Microfabricated immunoisolating biocapsules," *Biotechnology and Bioengineering*, vol. 57, pp. 118-120, 1998.
[22] A. Azam, K. E. Laflin, M. Jamal, R. Fernandes, and D. H. Gracias, "Self-folding micropatterned polymeric containers," *Biomedical Microdevices*, vol. 13, pp. 51-58, 2011.